ACS Macro Letters

Letter

pubs.acs.org/macroletters

Enhanced Fluorescence Properties of Poly(phenylene ethynylene)-Conjugated Polyelectrolytes Designed to Avoid Aggregation

Jan-Moritz Koenen,[†] Xuzhi Zhu,[†] Zhenxing Pan,[†] Fude Feng,[‡] Jie Yang,[†] and Kirk S. Schanze*[,†]

[†]Department of Chemistry and Center for Macromolecular Science and Engineering, University of Florida, P.O. Box 117200, Gainesville, Florida 32611-7200, United States

[‡]Baylor College of Medicine, Texas Medical Center, Houston, Texas 77030, United States

Supporting Information

ABSTRACT: A new class of nonaggregating conjugated polyelectrolytes exhibits efficient fluorescence in aqueous solution. Analysis by optical spectroscopy and transmission electron microscopy reveals a unique structure−property correlation between oxygen substitution and aggregation.

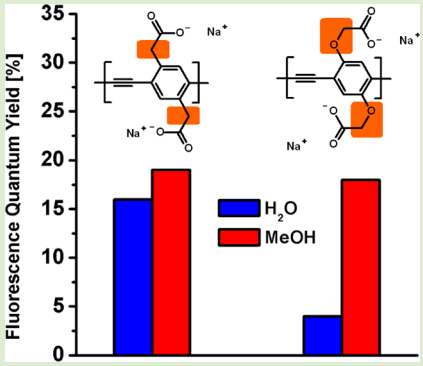

Conjugated polyelectrolytes (CPEs) feature a π-conjugated backbone and ionic side groups that make them soluble in polar solvents like water.[1,2] CPEs have been extensively studied in the past decade due to their possible applications as chemosensors,[3−5] biosensors,[3,6−8] injection barrier materials in organic light-emitting diodes,[9,10] or as the active layer in photovoltaic devices.[11,12]

Poly(*p*-phenylene ethynylene) (PPE) based CPEs have received special attention due to their remarkable fluorescence properties and facile synthesis via palladium-catalyzed Sonogashira coupling reactions.[13−15] On the basis of their propensity to undergo amplified fluorescence quenching, a variety of chemo- and biosensors based on PPE-type CPEs have been developed.[3,16] While the conjugated backbone in these systems is typically of the form $(-C\equiv C-\text{arylene}-)_n$, many different polar and ionic side chains have been investigated.[17−19] The polar, ionic side groups enable polymer solubility in polar solvents like water, while also introducing the possibility for ion-pair formation and/or selective binding with a specific analyte.[7,20] However, due to the rigid-rod and hydrophobic nature of the conjugated backbone, the solubility of CPEs in water is limited and often results in the formation of aggregate structures.[21,22] On the basis of the effect of aggregate-induced quenching, the fluorescence quantum yield of PPE-type CPEs is typically low in water ($\varphi \ll 10\%$).[22,23] The presence of aggregates has most often been inferred on the basis of photophysical results (i.e., red-shifted absorption and fluorescence spectra); however, in some cases direct evidence for CPE aggregate size and structure has been provided by dynamic light scattering (DLS),[24,25] fluorescence correlation spectroscopy (FCS),[26] electron microscopy,[27] and neutron scattering.[28,29]

We recently reported the synthesis and optical properties of a series of water-soluble PPE-type copolymers with branched side chains featuring three carboxylic groups per side chain.[30] This work found that the fluorescence yields of these CPEs were significantly higher than for corresponding polymers with linear ionic side chains with lower charge density. This effect was attributed to reduced aggregation and interchain interaction due to the higher charge density and the increased steric effect of the branched side chains.[30] Recently, Kim et al. reported the synthesis and photophysical properties of PPE-type polymers substituted with branched, oligo(ethylene glycol) (OEG) side chains that exhibit high fluorescence quantum yields in methanol and aqueous solutions ($\varphi > 30\%$). The high quantum yields were attributed to the long, bulky OEG side chains which decrease the tendency to form aggregates due to steric effects.[31] A similar effect was reported earlier for the structurally similar sulfonated polymers with branched OEG side chains.[32] In 2004, Aida et al. reported the synthesis of PPE-type CPEs that contained dendritic poly(benzyl ether) side chains of different generation.[33] These CPEs exhibited high fluoresence yields in water, with the values increasing with the generation number (size) of the dendritic side chains. This effect was also attributed to suppressed self-quenching by aggregation due to three-dimensional wrapping of the dendritic side chains around the polymer chains. Consideration of this previous work reveals

Received: January 31, 2014
Accepted: March 31, 2014
Published: April 8, 2014

   dx.doi.org/10.1021/mz500067k | *ACS Macro Lett.* 2014, 3, 405−409

that in the studies reported to date CPE aggregation has been suppressed via the use of bulky and/or highly charged side groups which prevent aggregation due to steric and/or charge repulsion effects.

In this letter we report the properties of a new class of PPE-type CPEs that display significantly enhanced fluorescence properties in water. Through structure−property correlation, we show that the enhanced fluorescence is surprisingly correlated with the absence of oxygen atom substitution on the phenylene rings. Detailed studies including fluorescence quenching, FCS, and transmission electron microscopy (TEM) suggest that the absence of the oxygen atom substitution decreases the tendency of the CPEs to aggregate in aqueous solution. Remarkably, bulky or highly charged side groups are not needed to suppress aggregation in these polymers. The findings are significant, as they reveal a new and straightforward approach to construction of water-soluble, nonaggregating highly fluorescent poly(phenylene ethynylene)-based CPEs. This work provides fundamental insight into molecular and electronic factors that contribute to CPE aggregation and will guide the design of polymers with enhanced photophysical properties in aqueous solution. Importantly, these properties are useful for the construction of sensitive and selective CPE-based fluorescence sensory systems.

Chart 1. Structures of the Polymer Series

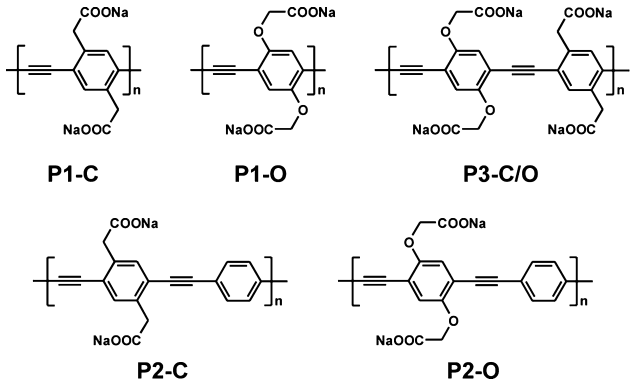

Five different PPE-type polymers were prepared in this study (Chart 1): two homopolymers P1−C and P1−O, two alternating phenylene copolymers P2−C and P2−O, and the alternating copolymer P3−C/O. All of these polymers share the same π-conjugated (1,4-phenylene ethynylene) backbone substituted with carboxylate ($-COO^-$) ionic groups; however, the structures differ in the linker used to connect the backbone to the ionic group (i.e., $-OCHH_2-$ (P1−O, P2−O) vs $-CH_2-$ (P1−C, P2−C) vs both (P3−C/O)).

The synthesis of P1−O and P2−O followed established methods starting with hydroquinone. The approach is straightforward and was used before in previous studies.[34,35] P1−C and P2−C were synthesized by a newly developed approach starting with 1,4-phenylenediacetic acid. As outlined in the Supporting Information, the polymers were constructed by palladium-catalyzed Sonogashira coupling of the ester-protected monomers. The corresponding CPEs were obtained by a subsequent base-assisted hydrolysis reaction and purification by dialysis against water (pH = 10). The molecular weights of the CPEs were estimated by GPC analysis of the ester-protected polymer precursors. All of the ester precursors have a molecular weight in the range of M_n = 12 000−20 000 g/mol and a polydispersity of PDI = 1.7−1.9. A table with the molecular weights M_n and M_w and the polydispersity is available in the Supporting Information.

The absorption and photoluminescence (PL) spectra of the two homopolyelectrolytes P1−C and P1−O as well as the three copolyelectrolytes P2−C, P2−O, and P3−C/O in water (pH = 8)[36] are depicted in Figure 1. The corresponding spectra in methanol can be found in the Supporting Information.

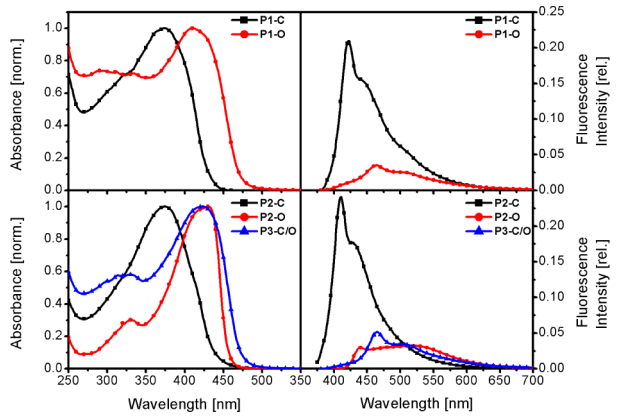

Figure 1. Absorption and fluorescence spectra of homopolymers P1−C and P1−O and copolymers P2−C, P2−O, and P3−C/O in water (pH = 8). Fluorescence spectra are area normalized corresponding to the relative quantum yields.

These solvents were selected based on previous work with structurally similar CPEs indicating that methanol is a good solvent (single polymer chains, minimal aggregation of the polymer) and water is a poor solvent (inducing aggregation of polymer chains).[22,23] The absorption maxima of all polymers lie between 374 and 430 nm. A significant red-shift of ≈30−50 nm is observed for the polymers that contain the oxygen linker (P1−O, P2−O, P3−C/O). This red-shift can also be observed for organic-soluble, alkoxy-substituted poly(phenylene ethynylene)s compared to the corresponding alkyl-substituted polymers.[37−40] The effect is attributed to the electronic donating effect of the alkoxy substituents which increases the HOMO energy and possibly decreases steric hindrance giving rise to more planar conformations of the backbone. Compared to the methanolic solutions, the absorption maxima of all polymers are slightly red-shifted in water.

Significant differences between the photoluminescence (PL) spectra of the CPEs in water can be observed. The emission maxima of the CPEs with oxygen linkers (P1−O, P2−O, P3−C/O) are red-shifted compared to the oxygen-free polymers (P1−C, P2−C). In addition, P1−C and P2−C exhibit a sharp emission band with a clear vibronic structure, whereas a broad emission of considerably reduced intensity is observed for P1−O, P2−O, and P3−C/O. The difference between the polymers becomes more evident when comparing the fluorescence quantum yields (Figure 2, also Table S1 in Supporting Information). While P1−C and P2−C have relatively high fluorescence quantum yields in water at ≈20%, the values for P1−O, P2−O, and P3−C/O are significantly less at ≈5%. Interestingly, all of the polymers exhibit a sharp and structured emission in methanol with comparable fluorescence quantum yields at ≈20% (Supporting Information). The emission maxima in methanol remain mostly the same except P2−O

dx.doi.org/10.1021/mz500067k | ACS Macro Lett. 2014, 3, 405−409

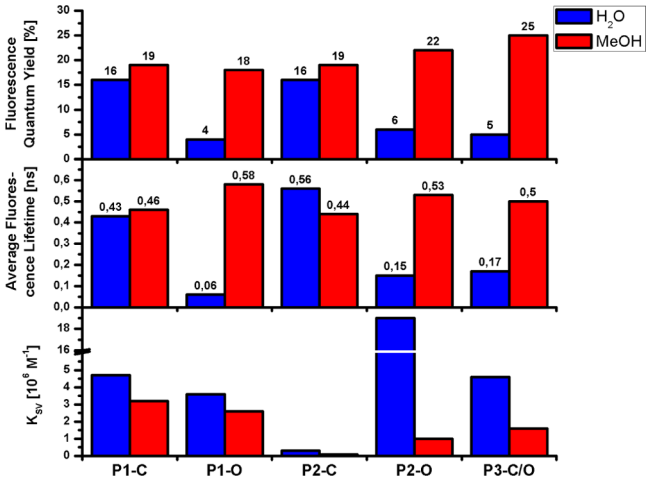

Figure 2. Fluorescence quantum yields (top, scale %), median fluorescence lifetimes (middle, $\langle\tau\rangle$, scale ns), and Stern−Volmer quenching constants (bottom, scale is $K_{SV}/10^6$ M^{-1}) in H_2O (blue) and MeOH (red).

which exhibits a 70 nm blue-shift compared to the emission maximum in water (Table 1, Supporting Information).

The fluorescence decays of the set of CPEs were measured by time-correlated single photon counting (TCSPC) in aqueous and methanol solutions. The median fluorescence lifetimes are depicted in Figure 1; more detailed results are available in the Supporting Information. A distinct difference between the polymers emerges: In methanol, the median lifetimes for all of the CPEs are comparable at ca. 0.5 ns. In contrast, the median lifetime in water remains the same for P1−C and P2−C, whereas for P1−O, P2−O, and P3−C/O, a 5-fold decrease in the lifetime to <0.1 ns in water is observed. The low fluorescence quantum yield and the short fluorescence lifetime of the polyelectrolytes P1−O, P2−O, and P3−C/O in aqueous solutions suggest that the rate of nonradiative decay is significantly enhanced for these polymers. On the basis of comparison of these results with previous studies, we suggest that the difference in properties between the C- and O-linked CPEs in water is related to their different tendency to form aggregates which act as exciton quenching sites.

To seek evidence supporting the hypothesis that the different optical properties observed for the O-linked CPEs in water arise due to the formation of aggregates, aqueous solutions of the polymers were analyzed by fluorescence correlation spectroscopy (FCS).[41,42] This method enables estimation of the average particle size by measuring the diffusion time of single fluorescent particles. The diffusion time was calibrated against an aqueous solution of fluorescein with known diffusion time (29.8 μs). Due to the limitations of FCS, these experiments were carried out with very low CPE concentration (2 μM in H_2O, pH = 8). The average diffusion times are listed in Table S1 (Supporting Information). Interestingly, the diffusion times in aqueous solutions are very similar in the range of 60−80 μs for all of the polymers except copolyelectrolyte P2−O. A significantly higher diffusion time of 223 μs is observed for this polymer, indicating the presence of large aggregates. On the basis of the diffusion times, the average particle sizes were estimated using a spherical model,[43] and the values are listed in the Supporting Information. These results suggest that under the conditions of FCS (low CPE concentration) only P2−O forms large aggregate structures. The results, however, do not preclude the existence of comparatively small aggregates for the other CPEs that may be in dynamic equilibrium with molecularly dissolved chains, therefore undergoing rapid exchange on the time scale of the FCS experiment, which is >10 μs.[44]

To gain more information about the aggregation state of the polyelectrolytes, samples prepared by evaporation of aqueous solutions of the polymers were imaged by transmission electron microscopy (TEM).[45] For the homopolymers P1−C and P1−O, samples deposited from 0.1 mM solution appear to give rise to relatively small, spherical aggregates (<10 nm, Figure 3a, 3b).

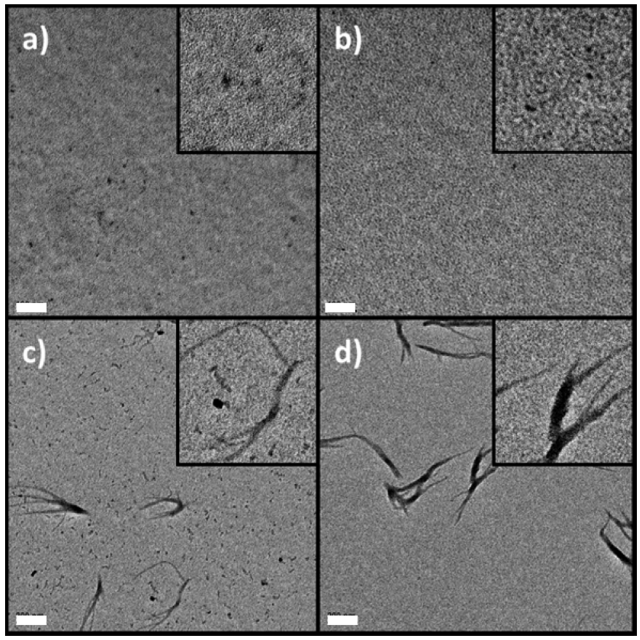

Figure 3. TEM images of samples deposited from aqueous solutions of (a) P1−C, (b) P1−O, (c) P2−C, and (d) P2−O. The samples were prepared by drop casting, followed by staining with aq. 1% PTA, and the concentration of the deposition solutions was 0.1 mM. Scale indicated by white bars in lower left of each image; for a, b 100 nm, for c, d 200 nm. Insets: approximately 5× magnification compared to the main image.

Interestingly, no significant difference between the two homopolymers is visible. By contrast, samples of copolymers P2−C and P2−O deposited from 0.1 mM solution form large aggregates which are readily visible (Figure 3c, 3d). These aggregates appear as "wormlike" structures that are 10−20 nm in width and length >100 nm.[46] Interestingly, an important difference can be seen in the images for P2−C and P2−O. In particular, for P2−C, in addition to the large wormlike aggregates, small elliptical or spherical shaped structures are also visible (size 10−20 nm). By contrast, these smaller structures are not seen in the images of P2−O (compare insets in Figure 3c and 3d). This finding suggests that the tendency to aggregate is less for P2−C, giving rise to a dynamic equilibrium between the small and larger structures.

Fluorescence quenching experiments on CPEs provide insight regarding the aggregation state of CPEs in solution.[7] In particular, aggregated CPE chains typically give significantly larger Stern−Volmer (SV) quenching constants (K_{SV}) compared to the same polymer in an unaggregated state.[34] In the present work we compared the SV quenching of the set of anionic CPEs with the cationic charge transfer quencher *N*,*N*′-

dx.doi.org/10.1021/mz500067k | ACS Macro Lett. 2014, 3, 405−409

dimethylviologen (MV^{2+}).[34] The quenching experiments were carried out in aqueous and methanol solutions. The quenching constants (K_{SV}) for each polymer are extrapolated from the linear region in the SV plots where the quencher concentration is very low, and the values are illustrated in the bar graph presentation in Figure 1c. In general, all of the polymers are quenched efficiently by MV^{2+} ($K_{SV} > 10^5$ M^{-1}), consistent with the "amplified quenching" effect.[22,23] However, close inspection of the data reveals interesting trends. First, the K_{SV} values for homopolymers P1−C and P1−O are similar at $\approx 3 \times 10^6$ M^{-1} in both methanol and water. By contrast, the fluorescence quenching of copolymer P2−C is ≈10 times less efficient in both solvents. The enhanced quenching efficiency of homopolymers P1−C and P1−O can be attributed to their higher charge density: each repeat unit is functionalized with two carboxylate groups, increasing the electrostatic attraction between the cationic quencher and the anionic polyelectrolytes.[47] Interestingly, the fluorescence quenching of P2−O in aqueous solution is 5 times more efficient compared to the homopolymers and 70 times more efficient than for P2−C. This increased quenching efficiency is remarkable since the charge density of P2−O and P2−C is the same. The increased quenching constant indicates that P2−O forms aggregates which can be more efficiently quenched by MV^{2+} than single polymer chains. By comparison, P2−C is not aggregated in water and has a low charge density, so the quenching is the lowest for this polymer.

Taken together, the results of fluorescence spectroscopy and quenching, FCS, and TEM reveal a distinct difference in the tendency of the series of CPEs to aggregate in water. The fluorescence studies, which are carried out at low polymer concentration, are clear in indicating that the −O− linked polymers P1−O and P2−O are aggregated in water, whereas $-CH_2-$ linked polymers P1−C and P2−C are not aggregated. However, the FCS, TEM, and quenching results are more complicated, revealing that P2−O is aggregated in all cases, whereas the situation for the other polymers is mixed.

We interpret these somewhat conflicting data as arising from several factors. First, the fluorescence-based experiments are carried out at low polymer concentration, where aggregation is less favored. By contrast, the TEM imaging work was conducted on samples deposited from 100-fold more concentrated solutions, which favors polymer aggregation. In addition, we believe that it is likely that there are different types of aggregates that are present in the polymer solutions (Scheme 1). Specifically, for a polymer solution there are three possible "states": (a) molecularly dissolved chains, (b) small aggregates (size <20 nm) consisting of just a few chains, and (c) large aggregates (size >50 nm) consisting of many chains. Importantly, the fluorescence-based techniques cannot distinguish between the large and small aggregate structures (the emission of both structures is dominated by the interchain exciton), while TEM imaging is only able to distinguish large aggregates. Thus, we suggest that in dilute aqueous solutions used for the fluorescence and FCS studies P1−C and P2−C are molecularly dissolved and that P1−O exists as small aggregates and P2−O as large aggregates. (The difference in the aggregate structures for the latter two structures arises because the lower charge density in copolymer P2−O favors the larger aggregate structures.)

Scheme 1. Proposed Process of Forming Aggregates: (a) Single Polymer Chains, (b) Small Aggregates (<20 nm) Containing Only a Few Polymer Chains, and (c) Large Polymer Aggregates (>20 nm) Containing Many Polymer Chains

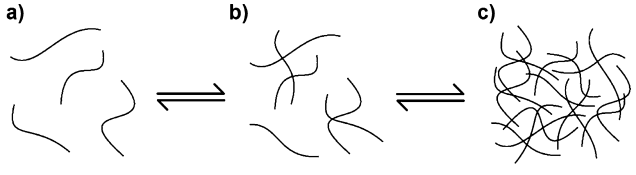

The important question to address is what causes the different aggregation behavior of the C- and O-linked CPEs? Careful consideration of the structures leads us to make several suggestions. One is that the oxygen substituents act through electronic effects. In particular, because the oxygen atoms are polar the O-substituted phenylene rings feature a quadrupole moment which could induce a weakly attractive interaction between dialkoxy-phenylene units in two chain segments. It is also possible that the electron-donating effect of the O-substituents can lead to a weakly attractive donor−acceptor interaction between chain segments (where an unsubstituted ring serves as the "acceptor"). On the other hand, we also consider the possibility that the oxygen substituents may facilitate chain aggregation through "nonelectronic" effects, e.g., by (1) allowing water molecules to stabilize a π-stacked arrangement via the formation of H-bond bridges between the O atoms on adjacent rings and/or (2) decreased steric interactions (relative to the $-CH_2-$ substituent) which facilitate a planarization of the phenylene ethynylene backbone.

Regardless of the molecular basis for the effect, the results presented herein are clear in demonstrating that in dilute aqueous solution the $-CH_2-$ linked CPEs (P1−C, P2−C) do not aggregate, whereas the −O− linked cogeners (P1−O, P2−O) are aggregated. This difference in solution properties leads to improved fluorescence properties (i.e., higher quantum yield, longer lifetime, and spectrally narrower bandshape) for $-CH_2-$ linked CPEs. This fundamentally interesting property may be used advantageously to create CPE-based chemo- and biosensors with improved selectivity and sensitivity.

EXPERIMENTAL SECTION

Corrected steady-state emission measurements were collected by a Photon Technology International (PTI) photon counting fluorescence spectrophotometer with optically dilute solutions. Fluorescence quantum yields were measured at RT in air-saturated solvents using quinine sulfate in 0.1 M aq. H_2SO_4 as a standard (Φ_{fl} = 0.54). Fluorescence correlation spectroscopy (FCS) measurements were obtained on a homemade setup using a 405 nm diode laser (Coherent, CUBE) as the excitation light.[41] Fluorescein (30 nM in 10 mM phosphate buffer, pH = 8) was used as the calibration for the system. The concentrations of oligomer and polymer samples are 5 μM.

Fluorescence lifetimes were obtained by a time-correlated single-photon counting technique (TCSPC) with a PicoQuant FluoTime 100 compact fluorescence lifetime spectrophotometer. A UV-pulsed diode laser provided the excitation at 375 nm powered by a pulsed diode laser driver (PicoQuant PDL800-B). The emission wavelength is selected by using 10 nm bandpass interference filters. Fluorescence decays were obtained at at least five wavelengths across the emission spectrum, and the data were analyzed by a global fit (PicoQuant FluoFit software). Fluorescence lifetimes were calculated from the global fit as average amplitude weighted from the fluorescence decays using biexponential fitting parameters. Reported median lifetime values were computed according to the expression $\langle\tau\rangle = \Sigma(\alpha_i \cdot \tau_i)$. All samples were prepared in air-saturated solvents.

dx.doi.org/10.1021/mz500067k | ACS Macro Lett. 2014, 3, 405−409

For the TEM images, aqueous solutions of the polymers were applied for 10 min onto the carbon surface of 400-mesh copper electron microscope grids (Ted Pella, covered with Formvar and carbon films) and washed with water. After staining with 1% phosphotungstic acid (PTA) (6 μL) for 2 min, the samples were washed with ethanol and air-dried. The grids were then examined on a Hitachi H-7500 Transmission Electron Microscope at a magnification of 10 000−50 000×. The images were analyzed with ImageJ software (version 1.46r).

■ ASSOCIATED CONTENT

Supporting Information

Complete details concerning the synthesis and characterization of monomers and polymers, including NMR spectra. Additional photophysical, fluorescence correlation spectroscopy, and dynamic light scattering data. This material is available free of charge via the Internet at http://pubs.acs.org.

■ AUTHOR INFORMATION

Corresponding Author

*E-mail: kschanze@chem.ufl.edu.

Notes

The authors declare no competing financial interest.

■ ACKNOWLEDGMENTS

We thank Prof. Jin Wang's group at the Department of Pharmacology and Dr. Michael Mancini at the Integrated Microscopy Core at Baylor College of Medicine (Houston, TX) for the collaboration on TEM imaging. We acknowledge the United States Department of Energy (Grant DE-FG02-03ER15484) for support of this work.

■ REFERENCES

(1) Jiang, H.; Taranekar, P.; Reynolds, J. R.; Schanze, K. S. *Angew. Chem., Int. Ed.* **2009**, *48*, 4300−4316.
(2) *Conjugated Polyelectrolytes: Fundamentals and Applications*; Liu, B., Bazan, G. C., Eds.; Wiley: New York, 2013.
(3) Zheng, J.; Swager, T. M. *Adv. Polym. Sci.* **2005**, *177*, 151−179.
(4) Zhao, X.; Liu, Y.; Schanze, K. S. *Chem. Commun.* **2007**, 2914−2916.
(5) Zhao, X.; Schanze, K. S. *Chem. Commun.* **2010**, *46*, 6075−6077.
(6) Ji, E.; Wu, D.; Schanze, K. S. *Langmuir* **2010**, *26*, 14427−14429.
(7) Thomas, S. W., III; Joly, G. D.; Swager, T. M. *Chem. Rev.* **2007**, *107*, 1339−1386.
(8) Li, K.; Liu, B. *Polym. Chem.* **2010**, *1*, 252−259.
(9) Seo, J. H.; Namdas, E. B.; Gutacker, A.; Heeger, A. J.; Bazan, G. C. *Appl. Phys. Lett.* **2010**, *97*, 043303.
(10) Duan, C.; Wang, L.; Zhang, K.; Guan, X.; Huang, F. *Adv. Mater.* **2011**, *23*, 1665−1669.
(11) Fang, Z.; Eshbaugh, A. A.; Schanze, K. S. *J. Am. Chem. Soc.* **2011**, *133*, 3063−3069.
(12) Ding, L.; Jonforsen, M.; Roman, L. S.; Andersson, M. R.; Inganäs, O. *Synth. Met.* **2000**, *110*, 133−140.
(13) Bunz, U. *Chem. Rev.* **2000**, *100*, 1605−1644.
(14) Sonogashira, K.; Tohda, Y.; Hagihara, N. *Tetrahedron Lett.* **1975**, *50*, 4467−4470.
(15) Sonogashira, K. *Organomet. J. Chem.* **2002**, *653*, 46−49.
(16) Liu, Y.; Ogawa, K.; Schanze, K. S. *J. Photochem. Photobiol. C* **2009**, *10*, 173−190.
(17) Wu, M.; Kaur, P.; Yue, H.; Clemmens, A. M.; Waldeck, D. H.; Xue, C.; Liu, H. *J. Phys. Chem. B* **2008**, *112*, 3300−3310.
(18) Clark, A. P.-Z.; Cadby, A. J.; Shen, C. K.-F.; Rubin, Y.; Tolbert, S. H. *J. Phys. Chem. B* **2006**, *110*, 22088−22096.
(19) Khan, A.; Müller, S.; Hecht, S. *Chem. Commun.* **2005**, 584−586.
(20) Kim, J.; McQuade, D. T.; McHugh, S. K.; Swager, T. M. *Angew. Chem., Int. Ed.* **2000**, *39*, 3868−3872.
(21) Pinto, M. R.; Kristal, B. M.; Schanze, K. S. *Langmuir* **2003**, *19*, 6523−6533.
(22) Tan, C.; Pinto, M. R.; Schanze, K. S. *Chem. Commun.* **2002**, 446−447.
(23) Zhao, X.; Pinto, M. R.; Hardison, L. M.; Mwaura, J.; Müller, J.; Jiang, H.; Witker, D.; Kleiman, V. D.; Reynolds, J. R.; Schanze, K. S. *Macromolecules* **2006**, *39*, 6355−6366.
(24) Jiang, H.; Zhao, X.; Schanze, K. S. *Langmuir* **2007**, *23*, 9481−9486.
(25) Schnablegger, H.; Antonietti, M.; Göltner, C.; Hartmann, J.; Cölfen, H.; Samori, P.; Rabe, J. P.; Häger, H.; Heitz, W. *J. Colloid Interface Sci.* **1999**, *212*, 24−32.
(26) Kaur, P.; Yue, H.; Wu, M.; Liu, M.; Treece, J.; Waldeck, D. H.; Xue, C.; Liu, H. *J. Phys. Chem. B* **2007**, *111*, 8589−8596.
(27) Burrows, H. D.; Tapia, M. J.; Fonseca, S. M.; Pradhan, S.; Scherf, U.; Silva, C. L.; Pais, A. A. C. C.; Valente, A. J. M.; Schillén, K.; Alfredsson, V.; Carnerup, A. M.; Tomsic, M.; Jamnik, A. *Langmuir* **2009**, *25*, 5545−5556.
(28) Förster, S.; Hermsdorf, N.; Böttcher, C.; Lindner, P. *Macromolecules* **2002**, *35*, 4096−4105.
(29) Claesson, P. M.; Bergström, M.; Dedinaite, A.; Kjellin, M.; Legrand, J.-F.; Grillo, I. *J. Phys. Chem. B* **2000**, *104*, 11689−11694.
(30) Lee, S. H.; Kömürlü, S.; Zhao, X.; Jiang, H.; Moriena, G.; Kleiman, V. D.; Schanze, K. S. *Macromolecules* **2011**, *44*, 4742−4751.
(31) Lee, K.; Kim, H.-J.; Kim, J. *Adv. Funct. Mater.* **2012**, *22*, 1076−1086.
(32) Lee, K.; Cho, J. C.; DeHeck, J.; Kim, J. *Chem. Commun.* **2006**, 1983−1985.
(33) Jiang, D.-L.; Choi, C.-K.; Honda, K.; Li, W.-S.; Yuzawa, T.; Aida, T. *J. Am. Chem. Soc.* **2004**, *126*, 12084−12089.
(34) Jiang, H.; Zhao, X.; Schanze, K. S. *Langmuir* **2006**, *22*, 5541−5543.
(35) Haskins-Glusac, K.; Pinto, M. R.; Tan, C.; Schanze, K. S. *J. Am. Chem. Soc.* **2004**, *126*, 14964−14971.
(36) Absorption and fluorescence experiments as a function of pH on P1−C and P1−O reveal that the pK_a values for the carboxylic acid units are in the range 5−6. At pH 8 all the polymers are fully ionized.
(37) Lebouch, N.; Garreau, S.; Louarn, G.; Belletête, M.; Durocher, G.; Leclerc, M. *Macromolecules* **2005**, *38*, 9631−9637.
(38) Davey, A. F.; Elliott, S.; O'Connor, O.; Blau, W. *J. Chem. Soc., Chem. Commun.* **1995**, 1433−1434.
(39) Swager, T. M.; Gil, C. J.; Wrighton, M. S. *J. Phys. Chem.* **1995**, *99*, 4886−4893.
(40) Bao, Z.; Chan, W. K.; Yu, L. *J. Am. Chem. Soc.* **1995**, *117*, 12426−12435.
(41) Chen, Y. *Analysis and Applications of Fluorescence Fluctuation Spectroscopy*; University of Illinois at Urbana-Champaign: Urbana, IL, 1999.
(42) Yang, J.; Wu, D.; Xie, D.; Feng, F.; Schanze, K. S. *J. Phys. Chem. B* **2013**, *117*, 16314−16324.
(43) Jameson, D. M.; Ross, J. A.; Albanesi, J. P. *Biophys. Rev.* **2009**, *1*, 105−118.
(44) Dynamic light scattering experiments carried out at higher concentration (0.1 mM) are consistent with the FCS results, showing that P2−O is strongly aggregated in water, and also suggest a greater tendency towards aggregation for P1−O vs P1−C. See Supporting Information, Figure S14.
(45) Solutions of the polymers with different concentration (0.001, 0.01, and 0.1 mM, polymer repeat unit concentration) were applied onto TEM grids. However, TEM images of the samples prepared from concentration <0.1 mM did not give rise to features that could be clearly imaged on the grids.
(46) Similar wormlike structures were previously reported in TEM images for a water-soluble PPE with only one carboxylic group per repeat unit; see ref 25.
(47) Feng, F.; Yang, J.; Xie, D.; McCarley, T. D.; Schanze, K. S. *J. Phys. Chem. Lett.* **2013**, *4*, 1410−1414.